Published online 30 September 2012: Nature Physics 8, 812

DOI: 10.1038/NPHYS2434

Self-organized electromagnetic field structures in laser-produced counterstreaming plasmas

N. L. Kugland[1] *, D. D. Ryutov[1], P.-Y. Chang[2], R. P. Drake[3], G. Fiksel[2], D. H. Froula[2], G. Gregori[4], M. Grosskopf[3], M. Koenig[5], Y. Kuramitsu[6], C. Kuranz[3], M. C. Levy[1,7], E. Liang[7], J. Meinecke[4], F. Miniati[8], T. Morita[6], A. Pelka[5], C. Plechaty[1], R. Presura[9], A. Ravasio[5], B. A. Remington[1], B. Reville[4], J. S. Ross[1], Y. Sakawa[6], A. Spitkovsky[10], H. Takabe[6], H.-S. Park[1]

1. Lawrence Livermore National Laboratory, Livermore, California 94550, USA
2. Laboratory for Laser Energetics, University of Rochester, Rochester, New York 14636, USA
3. Department of Atmospheric, Oceanic, and Space Sciences, University of Michigan, Ann Arbor, MI 48109, USA
4. Department of Physics, University of Oxford, Parks Road, Oxford OX1 3PU, UK
5. Laboratoire pour l'Utilisation des Lasers Intenses (LULI), École Polytechnique-Univ, Paris VI, 91128 Palaiseau, France
6. Institute of Laser Energetics, Osaka University, Osaka 565-0871, Japan
7. Rice University, Houston, Texas 77251, USA
8. Physics Department, Wolfgang-Pauli-Strasse 27, ETH-Zürich, CH-8093 Zürich, Switzerland
9. University of Nevada, Reno, 1664 N. Virginia Street, Reno, Nevada 89557, USA
10. Princeton University, Princeton, New Jersey 08544, USA

***Corresponding Author: Nathan Kugland (kugland1@llnl.gov, +1 925-422-3739)**

Self-organization is a topic of fundamental interest across physics, chemistry, and biology[1,2]. In plasmas, self-organization occurs when an inverse cascade progressively transfers energy from smaller to larger scales[3]. Global structures emerging from turbulent plasmas can be found in the laboratory[4] and in astrophysical settings such as the cosmic magnetic field[5,6], the collisionless shocks in supernova remnants[7], and the internal structures in Herbig-Haro (HH) objects[8]. Here we show for the first time that large, stable electromagnetic field structures can arise within counterstreaming supersonic plasmas in the laboratory. These surprising structures form by an unknown mechanism, are predominantly oriented transverse to the primary flow direction, extend for much larger distances than the intrinsic plasma spatial scales, and persist for much longer than the plasma kinetic time scales. Our results challenge existing models of counterstreaming plasmas and can be used to better understand large-scale and long-time plasma self-organization.

Our experiments were performed at the OMEGA EP laser facility, where two kilojoule-class lasers irradiated two polyethylene (CH_2) plastic disks that faced each other at a distance of 8 mm, creating a system of high-velocity laser-ablated counterstreaming plasma flows. The experimental details are described in Fig. 1 and in the Methods. At early times out to at least 8 ns, *intra*-jet ion collisions are known to be strong (due to relatively low particle thermal velocities) but *inter*-jet ion collisions are rare (due to relatively high flow velocities), permitting the evolution of both hydrodynamic and collisionless plasma instabilities ([9,10], and Table 1). We visualized the electric and magnetic field structures in the counterstreaming plasmas with short-pulse laser-generated proton beam imaging[11,12], taken from two orthogonal views in order to evaluate possible azimuthal symmetry of the field structures. After roughly 3 ns, caustics (large intensity variations[13]) in the proton images indicate the formation of strong field zones within the plasma, likely due to sharp structures with strong gradients, as reported in our invited article on proton imaging of electromagnetic fields[14]. By 4 ns, the features have changed dramatically into two large swaths of straight transverse caustics that extend for up to 5 mm. This extent is large compared to the fundamental scale lengths of the plasma (Table 1) such as the Debye length (5000 times larger) and the ion inertial length (nearly 100 times larger), indicating a high degree of self-organization. This organization proceeds up to a

spatial scale that is comparable to the size of the system (i.e. the disk separation). These caustics remain in place from 4 to 7 ns, the remaining duration of the experimental window, indicating a high degree of stability. This 3 ns lifetime is long compared to fundamental plasma time scales: 75,000 times longer than the electron plasma period, nearly 3,000 times longer than the ion plasma period, and >30 times longer than the flow crossing time across the ≈100 μm wide structure thickness. Scaled laboratory experiments have demonstrated significant potential to enhance our understanding of the generation and evolution of fields in galactic- and extra-galactic environments,[15–18] and may be able to help address several major outstanding questions in astrophysics. For example, large-scale magnetic fields have been observed in young stellar objects (YSOs)[19] and are believed to drive the formation of YSO outflows[20] and increase the order of the flow[21] . However, the precise role of electromagnetic fields in shaping the large-scale structure of the associated jets and HH objects is still unknown[8]. Additionally, laser-produced plasmas may be capable of collisionless shock formation[10,22,23]. The role of astrophysical magnetic field generation at shocks may affect protogalactic structure formation[18,24], a possibility that seems more likely since the existence of coherent fields in galaxies has been recently observed[25]. In all of these astrophysical objects, as in our experiment, large-scale field structures are clearly identified. As different plasma instabilities likely dominate each of these systems, our work should be considered as a test bed for studying the general physics of self-organization in plasmas.

The electromagnetic fields in the counterstreaming CH_2 plasmas are visualized in the proton image time sequence of Fig. 2. This side-view sequence, which was obtained over six separate shots in which the proton beam delay was steadily increased, shows at a glance how the fields evolve. We note that for this millimeter-scale plasma with density near 10^{19} cm^{-3} (areal density near 10^{18} cm^{-2}) the proton imagery is created purely by electric and magnetic fields, with only negligible collisional scattering of the proton beam.

At early times of 0.5 ns, Fig. 2 **a**, small plasmas expand in isolation away from the CH_2 targets. By 2.2 ns, Fig. 2 **b**, the dominant image features are general turbulence as well as fine striations (10 μm scale) that are oriented along the counterstreaming (vertical) axis. By 3.7 ns, Fig. 2 **c**, the bulk populations of the two plasmas have almost

met, and the turbulent features have sharpened into strong caustics[14], many circular with a spatial scale of roughly 0.5 mm, along with a hint of longer-range organization along the horizontal direction. The sharp, clear features in these proton images imply a dominant curtain structure of fields, or possibly the presence of several (but not too many) volumetric field structures within the field of view. The presence of volumetric structures on a small scale would only cause blurring[14].

At 4.0 ns, Fig. 2 **d**, the features have changed dramatically from general turbulence to a strongly self-organized regime with two large swaths of horizontal caustics separated by roughly 1.5 mm in the object plane. These features appear to be up to 5 mm long and stand in place from approximately 4 – 7 ns (Fig. 2 **d** – **f**). This long lifetime implies that the plasma field structures are in a stable steady state. As detailed in Fig. 3 **a**, there are nearly closed caustic contours connecting the two horizontal features, suggesting a cellular field structure. The horizontal swaths themselves consist of multiple caustics clustered together, as shown in Fig. 3 **b**. The field structures that create this feature are roughly axisymmetric about the vertical axis, since images from the orthogonal proton beam (not shown) look similar. The features have a generally bubbly appearance that might be caused by hydrodynamic turbulence or other instability mechanisms.

The positions of the caustics in Fig. 2 **d** remain the same for images with proton energies from 7 – 15 MeV (see Supplementary Fig. 1), indicating that: 1) the structures must change over a time that is longer than the proton beam temporal spread, roughly 100 ps; 2) the features are created by sharp field structures. Proton deflection angles α have a well-known scaling with the proton energy W, namely $\alpha \propto W^{-1}$ for electric deflections and $\alpha \propto W^{-1/2}$ for magnetic deflections[14]. However, proton caustics caused by sharp spatial structures possess a special stability in the high-magnification regime: the gross position of the caustic is insensitive to W, and only the positions of the individual caustic branches (which are too finely spaced to individually resolve) are sensitive to W[14].

In order to better understand the origin of the field structures, let us consider the "ingredients" that are present. We know that the jets interpenetrate and that collisional stagnation of the two flows cannot occur in the time window during which we have proton images, although collisions do occur[9]. Conditions are appropriate to support the growth of electrostatic and electromagnetic plasma instabilities[22,23,26,27]. Strong and rapid electron and ion heating occurs around 2.5 – 3.5 ns, raising both temperatures by more than an order of magnitude[9]. This heating impacts both the visibility of electrostatic structures for proton imaging (electrostatic proton deflection ~ electric field ~ T_e) and the plasma dynamics (sound speed ~ $T_e^{1/2}$). Indeed, the high temperature might explain the dominance of the caustic features, which have not been seen with such clarity in previous proton imaging experiments (see references in Ref. [14]). Intra-jet shocks are expected to be present and might contribute to the heating and formation of large-scale structure[28]. Electrostatic structures with potentials on the order of the electron temperature seem the most plausible, given that rather high magnetic fields (tens of tesla) would be required to create caustics in these proton images[14]. While large magnetic fields are produced at the laser spot[29], they are subsequently advected and volumetrically diluted during the plasma expansion[23]. Consequently, in the volume near TCC (see Fig. 1) the counterstreaming plasmas are essentially unmagnetized, an interesting regime that is not well explored. The main proton image caustic features are summarized in Table 2.

While the origin of the fields that create the horizontal swaths of caustics is still unknown, we can nevertheless present a phenomenological description. These swaths of caustics could be from planar field structures, or the rims of conical or cylindrical discontinuities, seen side-on. A central "blob" of field might exist, possibly with a cellular structure, in which the upper and lower edges are the most visible. Our detailed analysis of proton imaging[14] suggests that two widely separated layers of fields are required to create two widely separated swaths of caustics; for our experimental regime, a single field layer only produces a pair of very finely spaced caustics that appear as one on the detector. However, exact determination of the volume occupied by the fields (including the corresponding object plane sizes) will require additional experimental work: one might vary the proton source distance, film distance, and viewing angle.

Our work shows the emergence of large, stable, self-organized fields in counterstreaming plasmas. These structures persist for thousands of ion- and tens of thousands of electron-kinetic time scales. Although it is not entirely clear how these structures form, evidence of their existence is clearly seen in the experimental data. This highly non-linear regime appears to be beyond the reach of self-consistent simulations: at the present time, there are no three-dimensional simulations that can correctly resolve the non-linear plasma instabilities, ion kinetics, and structure formation to obtain agreement with the experimental results shown here.

Methods

The symmetric experimental configuration used two long-pulse (2200 J, 3 ns) 351 nm laser beams that focused with an intensity of approximately 9 x 10^{15} W/cm^2 (spot diameter roughly 100 μm) onto two 2 mm diameter x 0.5 mm thick CH_2 disk targets to create the counterstreaming plasmas. We performed proton imaging with two short-pulse (250 J, 10 ps) 1053 nm laser beams focused to 2 x10^{18} W/cm^2 onto two 2 mm diameter x 50 μm thick Au disk targets (only one is shown). These proton sources were located relatively far from TCC at a distance of 8 mm to use the entire ≈ f/1 proton beam to see from one CH_2 target to the other CH_2 target. (We consider the "object plane" to be the plane parallel to the proton source foil surface that passes through TCC.) Proton image magnification $M \approx 7.25$. Two 2.7 mm inside diameter Al washers covered with 3 μm thick Al foil protected the surface of the Au foil from perturbation by long-pulse CH_2 plasma[30]. To avoid interference, we delayed the two proton beams by 0.5 ns with respect to each other by staggering the short pulse laser timing. We collected the protons on radiochromic film layered with Al foil filters to obtain relatively narrowband images with protons from 5 to 15 MeV.

References

1. Ball, P. *The Self-Made Tapestry: Pattern Formation in Nature*. (Oxford University Press, USA: 1999).
2. Cross, M. C. & Hohenberg, P. C. Pattern formation outside of equilibrium. *Rev. Mod. Phys.* **65**, 851–1112 (1993).
3. Diamond, P. H., Itoh, S.-I. & Itoh, K. *Modern Plasma Physics: Volume 1, Physical Kinetics of Turbulent Plasmas*. (Cambridge University Press: New York, 2010).
4. Yamada, T. *et al.* Anatomy of plasma turbulence. *Nature Physics* **4**, 721–725 (2008).
5. Zweibel, E. G. & Heiles, C. Magnetic fields in galaxies and beyond. *Nature* **385**, 131–136 (1997).
6. Ryu, D., Kang, H., Cho, J. & Das, S. Turbulence and Magnetic Fields in the Large-Scale Structure of the Universe. *Science* **320**, 909–912 (2008).
7. Spicer, D. S., Maran, S. P. & Clark, R. W. A model of the pre-Sedov expansion phase of supernova remnant-ambient plasma coupling and X-ray emission from SN 1987A. *The Astrophysical Journal* **356**, 549 (1990).
8. Reipurth, B. & Bally, J. HERBIG-HARO FLOWS: Probes of Early Stellar Evolution. *Annual Review of Astronomy and Astrophysics* **39**, 403–455 (2001).
9. Ross, J. S. *et al.* Characterizing counter-streaming interpenetrating plasmas relevant to astrophysical collisionless shocks. *Physics of Plasmas* **19**, 056501–056501–8 (2012).
10. Park, H.-S. *et al.* Studying astrophysical collisionless shocks with counterstreaming plasmas from high power lasers. *High Energy Density Physics* **8**, 38–45 (2012).
11. Hatchett, S. P. *et al.* Electron, photon, and ion beams from the relativistic interaction of Petawatt laser pulses with solid targets. *Physics of Plasmas* **7**, 2076–2082 (2000).
12. Snavely, R. A. *et al.* Intense High-Energy Proton Beams from Petawatt-Laser Irradiation of Solids. *Phys. Rev. Lett.* **85**, 2945–2948 (2000).
13. Nye, J. F. *Natural Focusing and Fine Structure of Light: Caustics and Wave Dislocations*. (Institute of Physics Publishing: Bristol, 1999).

14. Kugland, N. L., Ryutov, D. D., Plechaty, C., Ross, J. S. & Park, H.-S. Relation between electric and magnetic field structures and their proton-beam images (invited). *Rev. Sci. Instrum. (submitted)* (2012).

15. Remington, B. A., Arnett, D., Drake, R. P. & Takabe, H. Modeling Astrophysical Phenomena in the Laboratory with Intense Lasers. *Science Magazine* **284**, 1488–1493 (1999).

16. Ryutov, D. *et al.* Similarity Criteria for the Laboratory Simulation of Supernova Hydrodynamics. *The Astrophysical Journal* **518**, 821–832 (1999).

17. Remington, B. A., Drake, R. P. & Ryutov, D. D. Experimental astrophysics with high power lasers and Z pinches. *Rev. Mod. Phys.* **78**, 755 (2006).

18. Gregori, G. *et al.* Generation of scaled protogalactic seed magnetic fields in laser-produced shock waves. *Nature* **481**, 480–483 (2012).

19. Ray, T. P. *et al.* Large-scale magnetic fields in the outflow from the young stellar object T Tauri S. *Nature* **385**, 415–417 (1997).

20. Hartigan, P., Frank, A., Varniere, P. & Blackman, E. G. Magnetic Fields in Stellar Jets. *The Astrophysical Journal* **661**, 910–918 (2007).

21. Gardiner, T. A., Frank, A., Jones, T. W. & Ryu, D. Influence of Magnetic Fields on Pulsed, Radiative Jets. *The Astrophysical Journal* **530**, 834–850 (2000).

22. Takabe, H. *et al.* High-Mach number collisionless shock and photo-ionized non-LTE plasma for laboratory astrophysics with intense lasers. *Plasma Physics and Controlled Fusion* **50**, 124057 (2008).

23. Drake, R. P. & Gregori, G. Design Considerations For Unmagnetized Collisionless-Shock Measurements In Homologous Flows. *The Astrophysical Journal* **749**, 171 (2012).

24. Kulsrud, R. M., Cen, R., Ostriker, J. P. & Ryu, D. The Protogalactic Origin for Cosmic Magnetic Fields. *The Astrophysical Journal* **480**, 481–491 (1997).

25. Bernet, M. L., Miniati, F., Lilly, S. J., Kronberg, P. P. & Dessauges-Zavadsky, M. Strong magnetic fields in normal galaxies at high redshift. *Nature* **454**, 302–304 (2008).

26. Kato, T. N. & Takabe, H. Nonrelativistic Collisionless Shocks in Unmagnetized Electron-Ion Plasmas. *The Astrophysical Journal* **681**, L93–L96 (2008).
27. Kato, T. N. & Takabe, H. Electrostatic and electromagnetic instabilities associated with electrostatic shocks: Two-dimensional particle-in-cell simulation. *Physics of Plasmas* **17**, 032114 (2010).
28. Ryutov, D. D. *et al.* Intra-jet shocks in two counter-streaming, weakly collisional plasma jets. *Phys. Plasmas* **19**, 074501 (2012).
29. Stamper, J. A. *et al.* Spontaneous Magnetic Fields in Laser-Produced Plasmas. *Phys. Rev. Lett.* **26**, 1012–1015 (1971).
30. Zylstra, A. B. *et al.* Using high-intensity laser-generated energetic protons to radiograph directly driven implosions. *Review of Scientific Instruments* **83**, 013511 (2012).

Acknowledgements. We thank the staff of the OMEGA EP laser facility for their experimental support. This work was performed under the auspices of the U.S. Department of Energy by the Lawrence Livermore National Laboratory, under Contract No. DE-AC52-07NA27344. Additional support was provided by LLNL LDRD Grant No. 11-ERD-054. Additional support came from the International Collaboration for High Energy Density Science (ICHEDS), supported by the Core-to-Core Program of the Japan Society for the Promotion of Science. The research leading to these results received funding from the European Research Council under the European Community's Seventh Framework Programme (FP7/2007-2013), ERC grant agreement no. 256973 and 247039.

Author Contributions. N.L.K. and H.-S.P. designed and prepared the experiment. The OMEGA EP experiments were carried out by N.L.K., H.-S.P., G.G., M.K., Y.K., J.M., T.M., A.P., C.P., J.S.R., and Y.S. The paper was written by N.L.K., D.D.R., and G.G. The data was analyzed by N.L.K. and D.D.R. Additional experimental and theoretical support was provided by P.-Y.C., R.P.D., G.F., D.H.F., M.G., C.K., M.C.L., E.L., F.M., R.P., A.R., B.R., A.S., and H.T.

Additional Information. Reprints and permissions information is available at www.nature.com/reprints. The authors declare no competing financial interests. Correspondence and requests for materials should be addressed to N.L.K. (kugland1@llnl.gov).

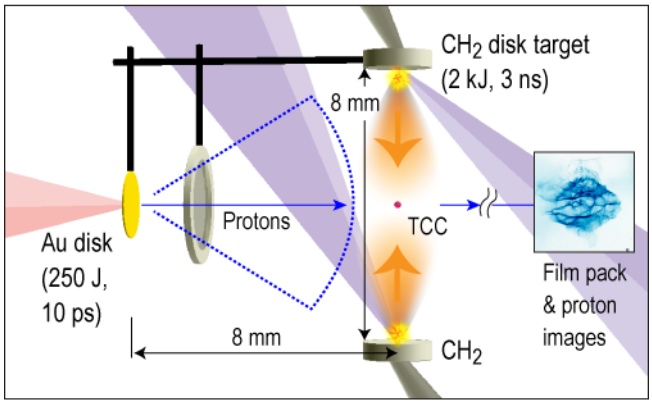

Figure 1 | Experimental setup at the OMEGA EP laser showing the targets, laser beams, and diagnostic configuration. Two long-pulse lasers created counterstreaming plasmas from CH_2 disk targets. The fields in these plasmas were visualized with short pulse laser-generated protons from two orthogonal views (only one line of sight is shown). The location of target chamber center (TCC) is marked with a pink dot. Typical radiochromic film data is shown in the inset image.

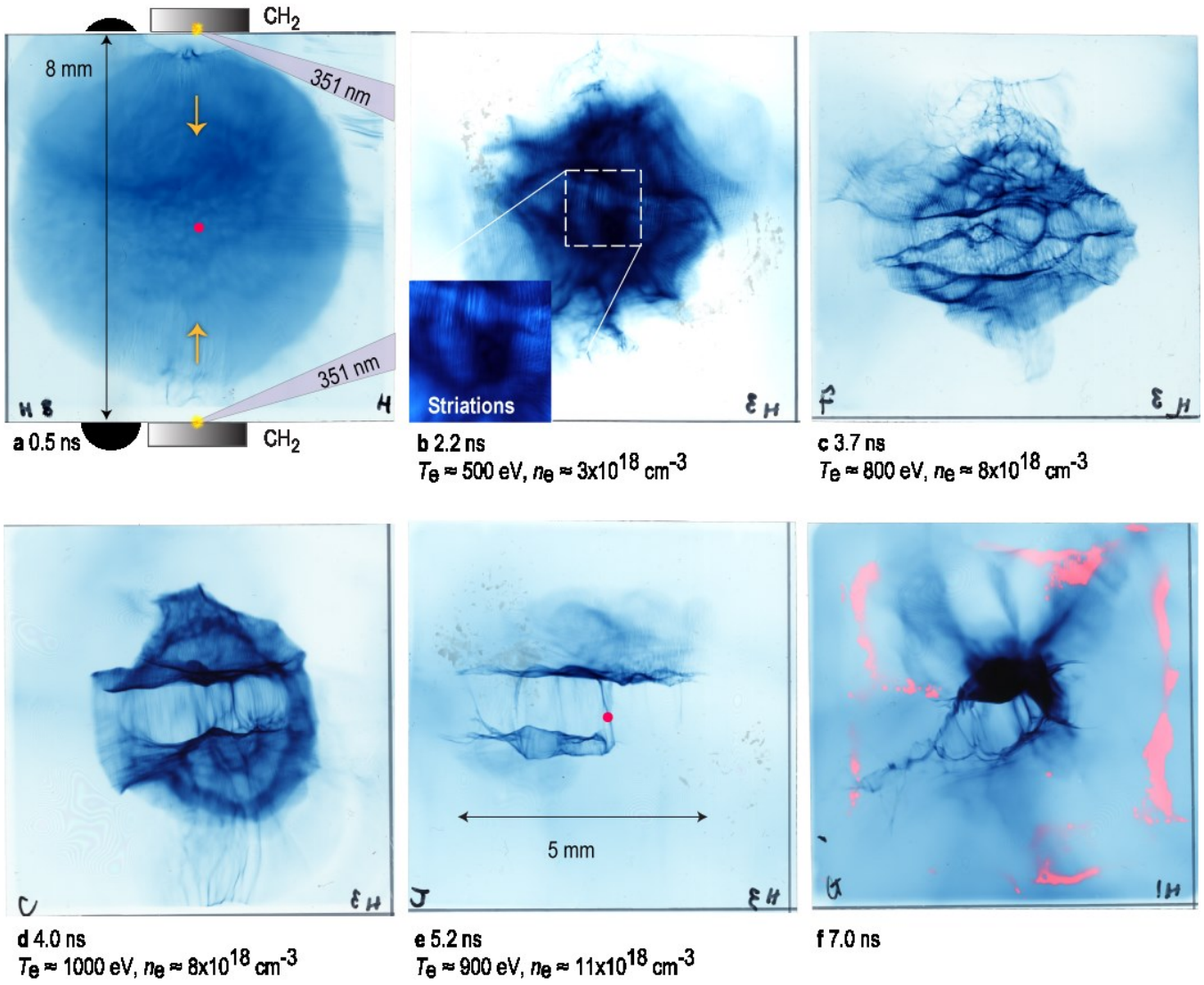

Figure 2 | Side-view time sequence of proton images showing the evolution of self-organized electromagnetic field structures. Dimensions are given in estimated object plane sizes. At the early time shown in panel **a**, the plasmas are still close to the targets, and the blotchiness in the center of the image is from weak modulations in the proton beam itself. Times indicated are when the protons in the center of each image reach TCC, i.e. the sum of the short pulse laser delay and the proton time of flight. Plasma parameters indicated are for TCC. Panels **a** through **e** have proton energy W=8.8 MeV; panel **f** has W=4.7 MeV. Image contrast has been individually adjusted. We measured the electron temperatures T_e and densities n_e at TCC with Thomson scattering (see Table 1).

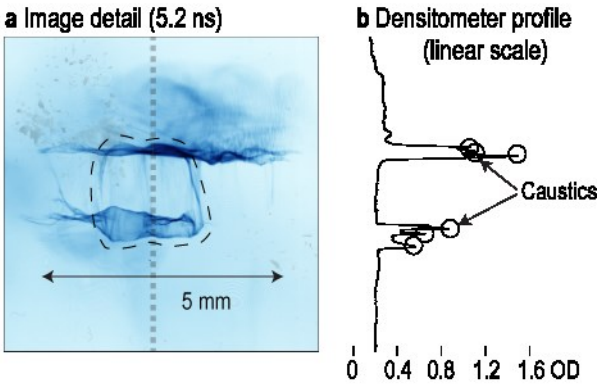

Figure 3 | Caustic detail. Panel **a** shows a detail of the proton image from Fig. 2 **d**, with the dashed line indicating a nearly closed contour suggestive of a cellular field structure. Panel **b** shows a line profile taken along the dotted line in panel **a**, from a separate scan of the film with a photometric densitometer.

Electron density n_e (cm^{-3})	**Electron Temperature** T_e (eV)	**Ion Temperature** T_i (eV)	**Flow velocity** v_{flow}
8×10^{18}	1000	1500	10^8 cm/s (1 mm/ns) Mach 3–5
***Inter*-jet collisional mean free path** λ_{mfp}	**Debye length** λ_{Debye}	**CH_2 ion plasma period** $\tau_{pi} = 2\pi/\omega_{pi}$	**CH_2 ion inertial length** c/ω_{pi}
250 mm (HH) 56 mm (CC)	0.1 μm	1.1 ps	51 μm

Table 1 | Typical plasma parameters for our counterstreaming CH_2 plasmas at 4 ns at TCC. We measured these with Thomson scattering at the OMEGA laser under similar target and laser conditions[9]. The mean free path listed is for ion-ion collisions between flows (*inter*-jet); HH and CC refer to hydrogen-hydrogen and carbon-carbon collisions, respectively. The fully ionized multi-species ion plasma frequency is calculated as $\omega_{pi}^2 = \omega_{pi[C]}^2 + 2\omega_{pi[H]}^2$, where the factor of 2 comes from the presence of two hydrogen atoms per carbon atom.

Caustic Feature	**Spatial Scale (object plane)**	**Most Visible**	**Possible origins**
Striations	10 um	2 ns	Shocks in a sheared flow
Turbulent circular caustics	0.5 mm	2-3 ns	Hydrodynamic instabilities (e.g. laser ablative or Rayleigh-Taylor)
Dual swaths of horizontal caustics	1 mm	4-7 ns	Requires a highly self-organizing inverse cascade mechanism. The outcome field structure could be dual planar, cylindrical/conical, or a single wavy blob
Nearly closed contours	1 mm	4-7 ns	Cellular field structures

Table 2 | Proton image features, properties, and possible origins.